Iranian Journal of Science & Technology, Transaction B, Engineering, Vol. 31, No. B3, pp 317-328
Printed in The Islamic Republic of Iran, 2007

A SELF-TUNABLE SENSORLESS METHOD FOR ROTOR POSITION DETECTION IN SWITCHED RELUCTANCE MOTOR DRIVES*

E. AFJEI,** O. HASHEMIPOUR, M. M. NEZAMABADI, AND M. A. SAATI

Dept. Electrical & Computer Engineering, Shahid Beheshti University, Saadat Research Institute, Tehran, I. R. of Iran, Email: E-afjei@sbu.ac.ir

Abstract– This paper presents the design of a complete self-tunable method for detecting the rotor position at low, high, and standstill speeds under different motor power ratings in a switched reluctance motor (SRM). In this method, high frequency diagnostic pulses with different pulse widths are applied to the three-stator pole windings and then the proper size pulse width is determined for that particular motor at standstill. At low speeds, the rotor positions are then sensed with the selected pulse width by applying the pulse to the un-energized phase winding while sensing the rotor position from the resulting phase winding current magnitude. At high speeds (beyond motor rated speed) the rotor position is detected by the current magnitude produced by the injected pulse and at the same time advancing the phase on time according to the motor speed. The designed controller is tested on different motor ratings ranging from 20 W to 2 KW. In order to demonstrate the feasibility and practicability of the method, this controller is applied in a vacuum cleaner with a switched reluctance motor.

Keywords– Switch reluctance motor, sensorless operation of SRM, indirect rotor position sensing in SRM, motor control

1. INTRODUCTION

The switched reluctance motor (SRM) is a very attractive and promising candidate in the area of variable speed drives for different applications used in the industry. The high performance of the SRM drive is dependent on the timing of the phase excitation in relation to the motor inductance profile, hence the rotor position information is essential for the proper operation of the motor. This objective has been traditionally achieved by utilizing a discrete shaft position sensor. Due to more ruggedness and greater reliability of the motor, especially in harsh environments, the trends for the past decades have been to eliminate the direct shaft position sensor. In this regard, different researchers have proposed a variety of indirect position-sensing techniques for the SRM drive. In all of the methods utilized, the information on the instantaneous phase inductance variation was used in some way or another to detect the rotor position indirectly. In general, the indirect rotor position sensing is obtained from the terminal measurements of the voltages, currents, and associated derivatives or, by injecting low-level high frequency signals into the non-energized phase inductance and then measuring the related outcomes [1]. Some of the indirect positions sensing methods cited in the literature are as follows:

a) Current magnitude and current waveform detection methods

As the motor turns, the inductance of each phase varies with the rotor position. The voltage pulses are placed on the non-energized phase windings and the resulting current magnitudes are measured and

*Received by the editors January 4, 2006; final revised form February 21, 2007.
**Corresponding author

compared to detect the rotor position. As in the current waveform detection method, the shape of the current or in other words, the gradient of the current is monitored to determine the rotor position [2].

b) Modulation techniques

In this technique, a high frequency carrier signal is injected to the non-energized phase. The signal containing the phase inductance information has a smaller frequency variation compared to the carrier signal and can be decoded using a demodulation technique to yield the rotor position. Some of the modulation techniques are AM, FM, and PM [3].

c) Flux-Current method

One of the simplest schemes is to measure the flux-linkage (λ), together with the phase current of the motor. Using these two formations and the non-linear static magnetization curve (λ, i, θ) of the motor, rotor position can be estimated. Flux is obtained by the following integration

$$\lambda = \int (v_{ph} - R.i_{ph})dt \tag{1}$$

Since the current goes to zero in every cycle, λ_0=0 can be used [4].

d) Observer based method

In this method, the state of the motor based on known system inputs are re-constructed and modeled in state space. The developed mathematical model runs in parallel with the real motor. Now, using the same inputs for both systems, the differences between the calculated and measured outputs are minimized. The position information produced by the mathematical model is used for the commutation of the actual motor [5].

e) Mutual voltage scheme

The principle of this technique is based on measuring the mutually induced voltage in an un-energized phase winding either adjacent or opposite to the energized phase. The magnitude of the induced voltage varies significantly as the rotor belonging to the energized phase moves from an un-aligned position to the full alignment. The mutually induced voltage in an adjacent pole is

$$v_m = \frac{d\lambda_m}{dt} = \frac{d(M(\theta)i)}{dt} = M(\theta)\frac{di}{dt} + i\frac{dM}{d\theta}\omega \tag{2}$$

where M(θ) is the mutual inductance and i is the phase current [6].

f) Intelligent-based estimation

There are different ways in the intelligent control methods such as artificial neural networks (ANN) [7-8] and fuzzy control [9-10] that have found applications in the detection of the rotor position in a switched reluctance motor. Neural networks have the inherent capability for identification. Rotor position estimation can be viewed as an identification process given the set of current and flux linkages from the three dimensional relationships that exist between them. Such an approach is used in the ANN-based rotor position estimator.

Fuzzy control uses a linguistic-based, approximated human reasoning to provide the solution to the problem of identification. The inputs are the estimated flux linkages and measured currents, and the output is the rotor position from which the speed is derived.

2. THE NOVEL METHOD

In order to come up with a technique to completely detect the rotor positions for the switched reluctance motor drives in all regions or modes of operation, the control scheme based on the motor torque-speed characteristics is used. Different researchers have also utilized the motor torque speed characteristics for the detection of the rotor position [11-13]. In this method, different motor ratings are connected to the same converter/controller circuit without any changes. Fig. 1 shows general torque-speed characteristics of a switched reluctance motor.

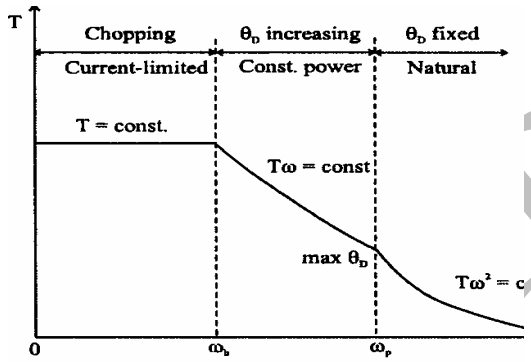

Fig. 1. General torque-speed characteristics and regions of SRM

In general, three regions of operation exist. The first region is known as the constant torque region, where the supply of voltage and commutation angles is fixed and is located below the rated speed, ω_b. The second region identified as the constant power region, starts from the rated speed ω_b. In this region applied voltage remains at its rated value and as the rated speed is increased, the maximum torque is sustained by advancing the turn on angle with a fixed commutation angle. In this region, the torque falls inversely to the motor speed, $1/\omega$. Finally, there is a practical limitation to advancing the turn on angle, which, lets say, begins at some speed called ω_p. At this point, the third region starts and the torque decreases as $1/\omega^2$. This mode is known as the natural mode and is usually neglected for most motor technology.

In order to control and run a SRM completely, three modes of operation, namely, standstill, low and high speeds are considered. The range of low speed begins at the motor start and ends at the rated speed ω_b, while the high speed commence at rated speed, ω_b, and goes up as much as the advancement of the turn on angle permits. Fig. 2 shows the control block diagram of the whole control system, which produces a self-tunable diagnostic pulse train for detecting the rotor position in the three modes of operation, as well as the automatic control of the motor speed in these regions.

The control block diagram can be explained briefly in the following manner. First is the 89C51 type microcontroller which receives and analyzes the input signals and makes the proper decisions for the correct motor phase selection. The second part is the receiving and processing section which consists of analog switches, an A/D converter and amplifiers. The analog switches get the information from each phase and then, by the use of multiplexing, sends the signals to the amplifier and then to A/D converter to be used by the microcontroller. Third is the PWM generator, which gets its input from the motor speed and generates the proper pulse-width. Fourth is the logic gate unit, which combines the microcontroller output signals and the PWM generator to produce the proper signals for the power switches. Finally, there is the two per phase switches power converter to deliver the necessary power to the motor. This system goes from one mode to the other mode of operation automatically according to the rated speed and vise versa. The user must set the rated and final speeds. The general voltage equation governing the phase winding is expressed as [11]:

$$V = Ri + \frac{\partial \lambda}{\partial \theta}\frac{d\theta}{dt} + \frac{\partial \lambda}{\partial i}\frac{di}{dt} \tag{3}$$

in which V, R, λ, and θ, denote phase voltage, phase resistance, flux linkage, and rotor position, respectively. The dynamic voltage equation for each region of torque speed characteristics is deduced from equation (3). It is important to notice that, the dynamic characteristics of the motor changes for every mode of operation, therefore the appropriate pulse width for that mode is generated.

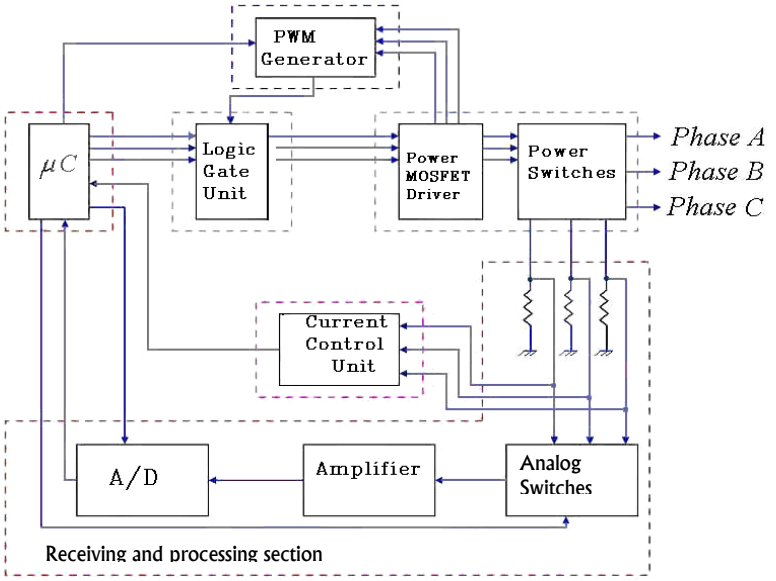

Fig. 2. The block diagram for the motor control

At this point, the different modes of operation are explained in which the first mode of operation starts at standstill.

The switched reluctance motor used for the vacuum cleaner has the following

specifications:

stator core outer diameter	= 72	mm
stator core inner diameter	= 62	mm
rotor pole arc	$=32^{o}$	
stator pole arc	$=28^{o}$	
stack length	=35	mm
airgap	= 0.25	mm
rotor core outer diameter	= 39.5	mm
rotor shaft diameter	= 10	mm
number of turns per pole	= 65	

In the numerical part, the magnetic field analysis is performed using a commercial finite element package [14], which is based on the variational energy minimization technique to solve for the magnetic vector potential. This simulation directly yields the prediction of flux linkages. The so-called "effective" inductance has been defined as the ratio of each phase flux linkages to the exciting current (λ / I). Values based on this definition are presented in Fig. 3 for the motor under investigation. In the analysis, the rotor moves from unaligned (i.e. 0^{o}) to aligned (i.e. 28^{o}) positions, and all "effective" inductance values for points in between are computed.

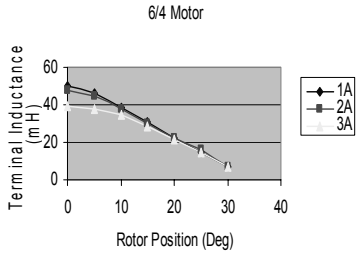

Fig. 3. Terminal inductance *vs*. rotor position

a) First mode of operation

At this point, the diagnostic pulses with proper widths are produced. In order to do this task, we start with the minimum pulse width generated by the microcontroller. These pulses are applied to the three motor phases and then the resulting currents are measured and added together. The phase voltage Eq. (1), in the absence of motional back EMF and saturation, are represented by the following equation:

$$V_A = [R + \frac{dL(\theta)}{dt}]i_A + L_A(\theta)\frac{di_A}{dt} \tag{4}$$

Where, V_A , i_A are phase A voltage pulse and the resulting current.
The solution to the above equation can be easily determined as:

$$i_A = \frac{V_A}{R^*}(1 + e^{-\frac{t}{\tau}}) \tag{5}$$

$$\text{Where, } R^* = R + \frac{dL(\theta)}{dt}, \text{ and } \tau = \frac{L_A(\theta)}{R^*}$$

The equations for the other phases have the same general form. The addition of the phase currents yields the same value for the summation and is independent of the rotor position. This can be readily verified by summing the three phase currents, which results in the following:

$$i(\tau) = \frac{V_A}{R^*}(3 - e^{-\frac{\tau}{L_1/R^*}} - e^{-\frac{\tau}{L_2/R^*}} - e^{-\frac{\tau}{L_3/R^*}}) \tag{6}$$

Where, L_1, L_2, L_3 are the phase inductances and τ stands for the duration of the diagnostic voltage pulse.
Notice that, at any rotor position, $L_1 + L_2 + L_3$ = constant= L_{max} and the L's have the following general form, $L_i = L_{min}$, $L_j = M\, L_{max}$ $L_k = (1\text{-}M)\, L_{max}$, where, i, j, k are the phase numbers, and,
M= (stator and rotor poles overlapped area) / (full aligned overlapped area),
hence, $0 \le M \le 1$.

Substituting for L's in (6) will always yield the same value for i(τ). A portion of this current, based on the system hardware, is used as a reference value for the comparison of each phase current for the detection of the rotor position. Now the pulse-width is increased by a pre-defined value and the same measurement is repeated as before. This process continues until the produced current from each phase has reached to a certain value in which the difference in current magnitudes for the phases can be completely identified by the sensing device, and also the motor has not moved from its starting position. In other

words, the torque produced by the pulses are insignificant. The rotor movement is verified by applying the same pulses with the selected pulse width three times to the motor phases and then measuring the outcomes. If the rotor has not moved, then the resulting current values produced by the tests must remain the same. If the rotor movement is detected, then the magnitude of the pulse is reduced and the tests are repeated again. Now, the diagnostic pulse with the proper pulse width is produced. Fig. 4 shows the diagnostic pulse train (b), and the resulting current pulses (a), from one of the motor phases.

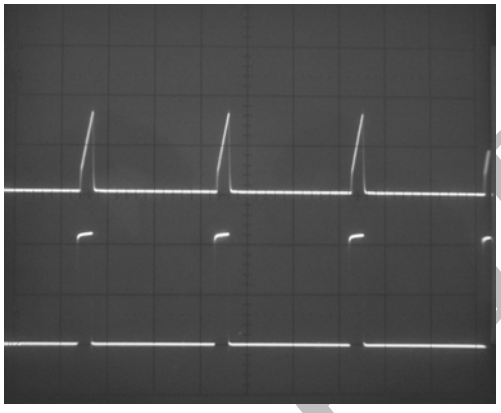

Fig. 4. a) The resulting current pulses from one of the motor phases.
b) Diagnostic pulses, timing 0.2 msec/div

The diagnostic pulses are applied to the coil windings of each phase. In order to detect the proper motor phase, the resulting current magnitudes of the corresponding phase and the direction of rotation are considered. It is noteworthy to mention that, the more aligned the rotor pole with respect to the stator poles, the higher the phase inductance, and therefore the lower the phase current magnitude. Fig. 5 shows the diagnostic pulse train and the resulting current pulses from the three motor phases.

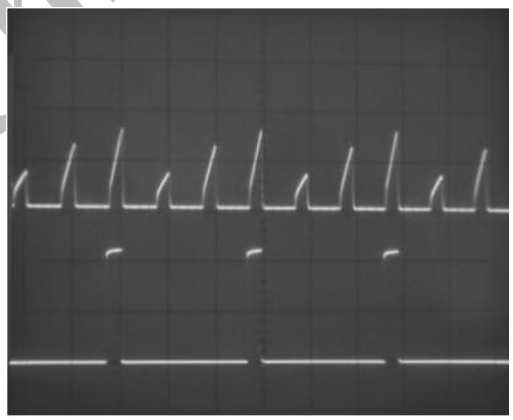

Fig. 5. a) The resulting current pulses from the motor 3 phases
b) Diagnostic pulse train, timing at 0.2 msec/div

The different resulting current magnitudes are due to the different motor phase inductances. Fig. 6 shows the flow chart for the detection of the rotor position.

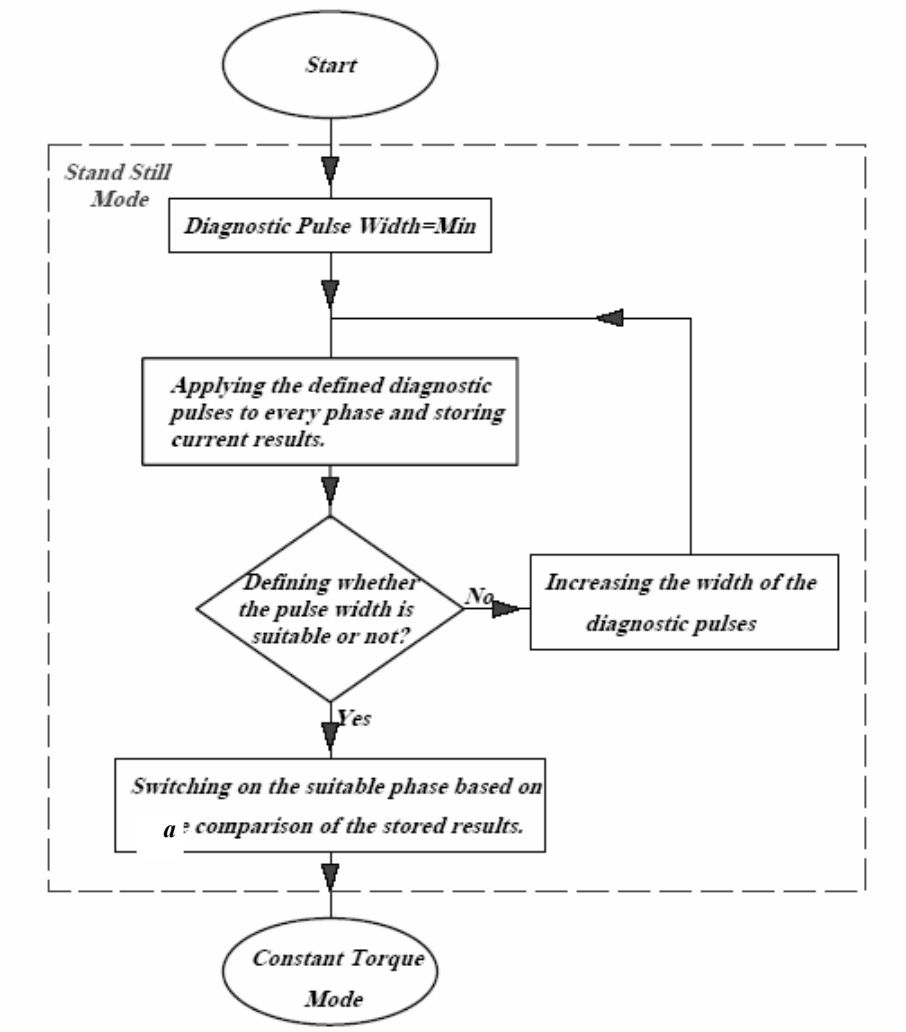

Fig. 6. The flow chart for the stand still mode of operation

Now the motor starts turning and the next mode of operation begins.

b) Second mode of operation

In this mode, the motor begins to turn. Figure 7 shows the front view of a three phase switched reluctance motor with the coils all marked as AA′ , BB′, and CC′ belonging to phases A, B, and C, respectively.

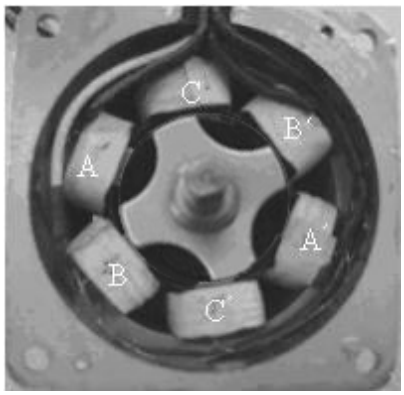

Fig. 7. The front view of a three phase motor

As shown in Fig. 7, phase A is in a fully unaligned position, while phases B and C are in almost half aligned positions. To restate, phase A is off and one of the two remaining phases due to the direction of rotation is on. If a clockwise direction is considered, then phase C is on at this time and phase A is the one next in line to be turned on. In this mode, the diagnostic pulses are applied to only one of the un-energized phases that can provide the most information about the rotor position and has no free wheeling current flow. In this case, phase A, shown in Fig. 7, is the right one for this job. The simplified version of the phase A voltage equation in this mode will have the following form:

$$V_A = [R + \omega \frac{\partial L(\theta)}{\partial \theta}] i_A + [L_A(\theta) + i_A \frac{\partial L(\theta)}{\partial i}] \frac{di_A}{dt} \tag{7}$$

The solution to Eq. (7) yields the following result for the resulting phase current, i_A

$$i_A = \frac{V_A}{R^*} + [I_0 - \frac{V_A}{R^*}] e^{-\frac{t}{\tau}} \tag{8}$$

Where, I_0 is the initial current, $R^* = R + \omega \frac{\partial L(\theta)}{\partial \theta}$, $L^* = L_A(\theta) + i_A \frac{\partial L(\theta)}{\partial i_A}$, and $\tau = \frac{L_A^*}{R^*}$.

As the rotor pole passes from the mid un-aligned position shown in Fig. 5 and gets closer to phase A of the stator poles, the magnitude of the current pulses resulting from the injection of the diagnostic pulses on that phase starts from a maximum value at a mid un-aligned position and decreases to a minimum value at a fully aligned position. This corresponds to a 45 degree rotor movement. Therefore, knowing the minimum and the maximum values of the current pulses, one can obtain the proper rotor position to turn on the corresponding motor phase. The motor dynamic characteristics are different than the pervious mode, therefore the same pulse-width might not be suitable for this mode of operation, and as the motor speed changes, the width of the pulse train must be continuously modified. In this mode, the width of the pulse is reduced according to the motor speed and the input voltage in such a way that the resulting maximum current magnitude reaches a pre-set value. This value is determined by the system hardware so that the input to the A/D converter stays in the specified range. Figure 8 shows the diagnostic pulses, the resulting current pulses, as well as the gate command for the phase turn on before being shaped and magnified by the amplifiers.

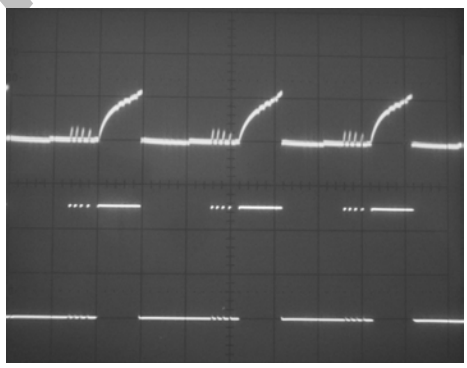

Fig. 8. a) The resulting current pulses, b) The gate commands, timing at 0.5 msec/div

As seen from Fig. 8, the magnitudes of the resulting current pulses decrease as the rotor pole gets closer to the stator pole of the corresponding phase. When the current magnitude reaches a certain pre-determined range, the gate command to energize the proper phase is activated. In order to get proper and sharp gate signals for the converter power transistors, the current signals are shaped and magnified as shown in Fig. 9.

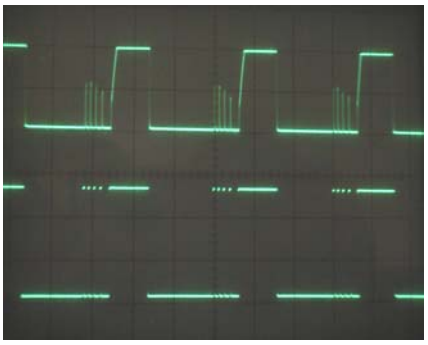

Fig. 9. a) Resulting shaped and magnified current signals,
b)The gate commands, timing at .5 msec/div

As shown in Fig. 9, the magnitude of the current pulses are clearly increasing and then decreasing as the rotor poles align themselves with the corresponding stator poles.

In this mode of operation, the motor speed is varied by the PWM technique. When the duty cycle of the PWM reaches 100 percent, the next mode of operation begins. Fig. 10 shows the complete flow chart for the constant torque mode.

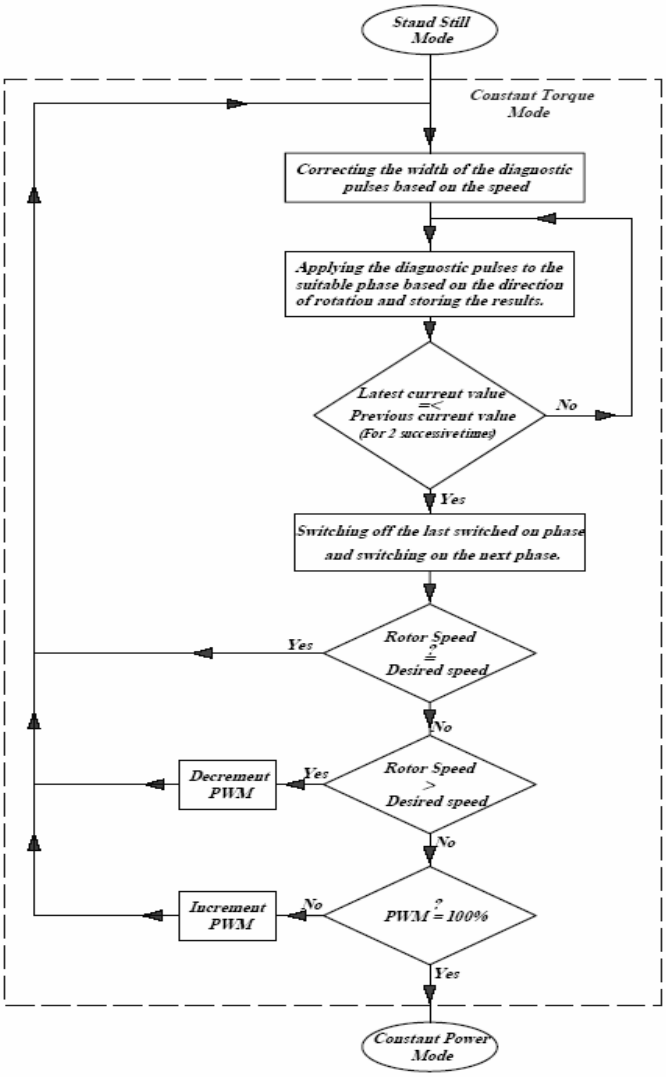

Fig. 10. The flow chart for the constant torque mode of operation

c) Third mode of operation

This mode corresponds to the second and third parts of the torque-speed characteristics of the motor shown in Fig. 1 known as constant power and natural regions.

As motor speed increases, the shape of the current waveform changes in such way that the production of the motoring torque is limited. At high speeds, it is possible for the phase current to never reach the desired value due to the self-e.m.f. of the motor, therefore the torque falls off. In order to remedy this problem and produce high speeds, the phase turn on angle is advanced in such a way that the phase commutation begins sooner. Advancing the commutation angle offers the advantages of getting the current into the phase winding while the inductance of the phase is low, and also of having a little more time to get the current out of the phase winding before the rotor reaches the negative torque region. Since the SRM drive is a variable speed motor, the amount of advancing for the turn on angle should be accomplished automatically according to the speed of the motor, meaning, as the motor speed increases, so should the turn on angle and vice versa.

In this mode, again diagnostic pulses are applied to the phase which is in an off state and also, its coils are not in discharging (free wheeling) mode. In this mode, the width of the pulse train is continuously monitored and modified, like in the previous mode.

The resulting current pulses flowing in phase A are deduced from the following voltage equation:

$$V_A = R.i_A + L(\theta)\frac{di}{dt} + i_A \frac{dL(\theta)}{d\theta}\omega \tag{9}$$

where, V_A and i_A are phase A voltage and current, respectively R and L are resistance and inductance of the phase ω is the motor speed. The solution to Eq. (9) yields the following result for the current, i_A

$$i_A = \frac{V_A}{R + \frac{dL}{d\theta}\omega} + [I_0 - \frac{V_A}{R + \frac{dL}{d\theta}\omega}]e^{-\frac{t}{\tau}} \tag{10}$$

Where, I_0 is the initial current at the beginning of each step, and $\tau = \dfrac{L(\theta)}{R + \dfrac{dL(\theta)}{d\theta}\omega}$.

It is possible to find the solution to Eq. (10) numerically for different time steps within the width of the pulse. A feedback from the motor speed is fed into the microcontroller to generate proper advancement. Using the information from the magnitude of the resulting current pulses and the amount of advancement, the phase turn on command is generated. This process continues until the speed reaches the set value. Figure 11 shows the diagnostic pulses and the resulting current pulses, as well as the command for the phase turn on after being shaped and magnified.

Finally, Fig 12 shows the gate signals for the two consecutive phases. In this figure, the diagnostic pulses are also clearly shown just before the gate is turned on.

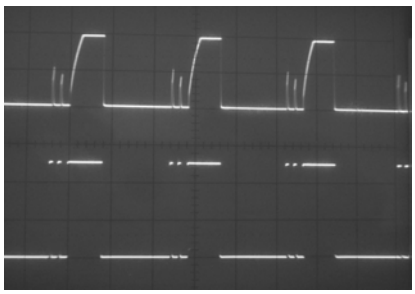

Fig. 11. a) The resulting shaped and magnified current signals,
b) The gate commands timing at 0.2 msec/div

Due to the high speed of the motor, there are two pulse samples shown in Fig. 12. Since the motor is three phase, each gate pulse is on for one third of the whole period. Fig. 13 shows the complete flow chart for the constant power mode.

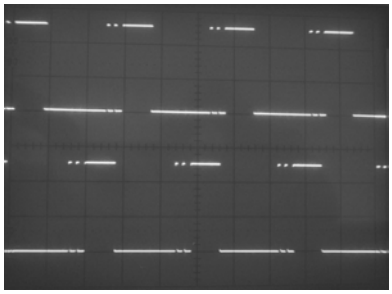

Fig. 12. Diagnostic pulses and gate pulses for two consecutive phases

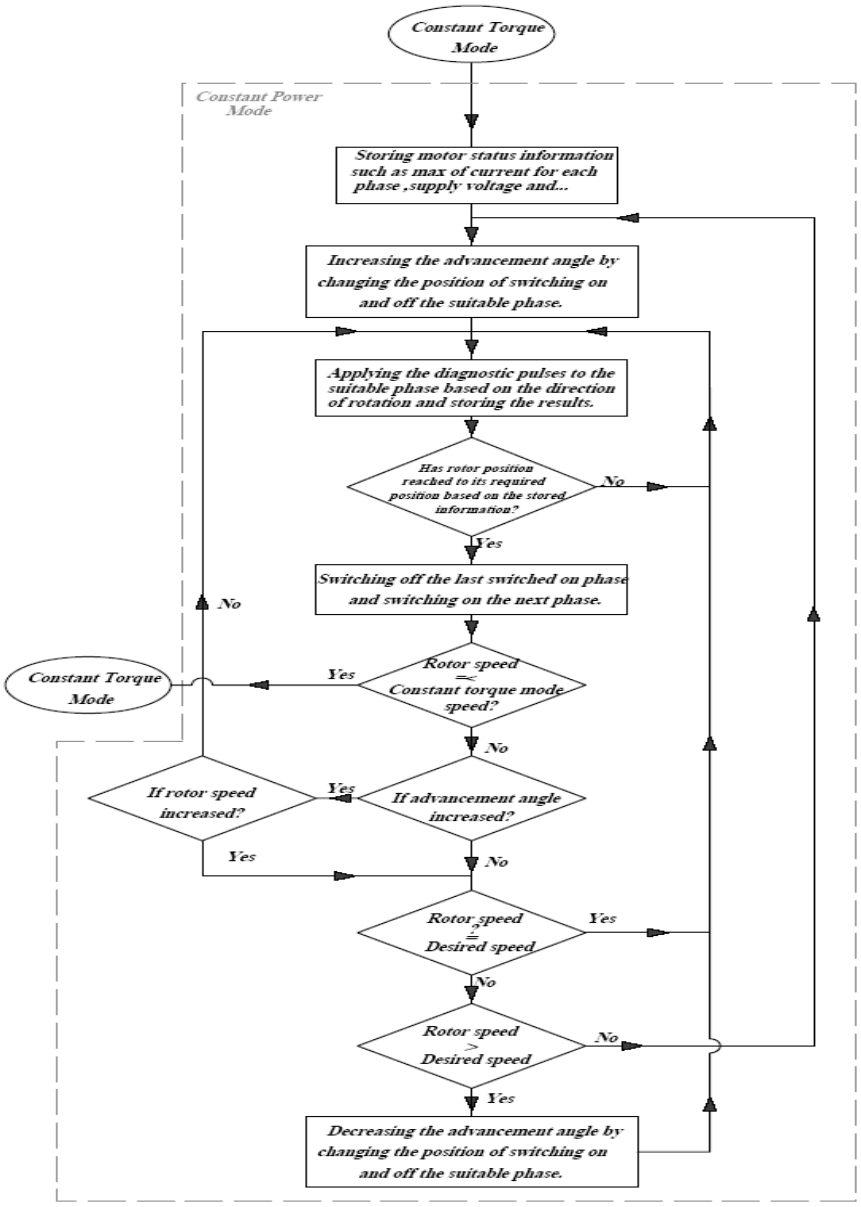

Fig. 13. The complete flow chart for the constant power mode

3. CONCLUSION

This paper has presented a complete self-tunable method designed to detect the rotor position at standstill, low, and high speeds in switched reluctance motors for different motor power ratings.

This technique has been tested successfully on a 6 by 4 SRM used as the driving force for a vacuum cleaner. The speed of the motor starts from zero and goes up to 20000 rpm. A pulse train is produced in the first mode of operation. It is continuously monitored in the different modes of operation for possible correction and modification of the pulse-width for the proper and quick detection of the rotor position. The method works fine in conjunction with the pulse width modulation used to control the motor speed in the constant torque region. The constant power region starts at 5000 rpm from this point on the turn on angle, begining the advancement according to the motor speed. The maximum advancement is about 15 degrees for the motor. The controller and drive circuit have also been tested on different switched reluctance motor power ratings (20 W- 2 KW) to check the reliability of the method and to ensure there are no unseen problems. The robust performance obtained from this method makes it an attractive candidate for industrial and domestic applications.

REFERENCES

1. Perl, T., Husain, I. & Elbuluk, M. (1995). Design trends and trade-offs for sensorless operation of switched reluctance motor drives. *Ind. Appl. Conf., 1995. Thirtieth IAS Annual Meeting, IAS '95, Conference Record of the 1995 IEEE.* Oct., Akron Univ., OH, USA, 278-285.
2. Acarnley, P. P., Hill, R. J. & Hooper, C. W. (1985). Detection of rotor position in stepping and switched reluctance motors by monitoring current waveforms. *IEEE Trans. Industrial Electronics, IE–32*(3) 215-222.
3. Ehsani, M., Husain, I., Mahajan, S. & Ramani, K. R. (1994). New modulation techniques for rotor position sensing in switched reluctance motors. *IEEE Trans. on Industry Applications, 30*(1), 85-91.
4. Lyons, J. P., MacMinn, S. R. & Preston, M. A. (1999). Flux/Current methods for SRM rotor position estimation. *IEEE–IAS Conf. Rec*., 482-487.
5. Husain, I., Sodhi, S. & Ehsani, M. (1994). Sliding mode observer based control for switched reluctance motors. *IEEE-IAS Conf. Rec*., 635-643.
6. Husain, I. & Ehsani, M. (1994). Rotor position sensing in switched reluctance motor drives by measuring mutually induced voltages. *IEEE Tran. On Ind. Appl., 30*(3), 665-672.
7. Bellini, A., Filippetti, F., Franceschini, G. Tassoni, C. & Vas, P. (1998). Position sensorless control of a SRM drive using ANN techniques. *Conf. Rec. IEEE Ind. Appl. Soc., Oct*., 709-714.
8. Mese, E. & Torrey, D. A. (1997). Sensorless position estimation for VR machine using artificial neural networks. *Conf. Rec. IEEE Ind. Appl. Soc., Oct*., 540-547.
9. Wang, Z., Cheok, A. D. & Wee, L. K. (2001). Sensorless rotor position estimation algorithm for switched reluctance motors using fuzzy logic. *Proc. Power electronics Specialist Conf., 3*, Cairns, Australia, June 7, 1701-1706.
10. Krishnan, R. (2001). *Switched Reluctance Motor Drive: Modeling, simulation, analysis, design and application*. Magna physics publishing.
11. Fahimi, B., Emadi, A. & Sepe, R. B. (2005). Four-quadrant position sensorless control in SRM drives over the entire speed range. *IEEE Trans. on Power electronics, 20*(1), 154-163.
12. Housain, S., Husain, I., Klode, H., Omekanda, A. & Gopalakrishan, S. (2003). Four quadrant and zero speed sensorless control of switched reluctance motor. *IEEE Trans. Ind. Appl., 39*(5), 1343-1349,
13. Ehsani, M. & Fahimi, B. (2002). Elimination of position sensors in Switched Reluctance Motor Drives: State of the Art and Future Trends. *IEEE Trans. on Industrial Electronics, 49*(1), 40-47.
14. Magnet CAD Package: *User Manual*, (2001). Infolytica Corporation Ltd. Montreal, Canada.